



**LUND UNIVERSITY**  
Faculty of Science

## Simulating electron transport in nanowires with imperfections using 'kwant'

Alexandros Pallas

---

Thesis submitted for the degree of Master of Science  
Project duration of 4 months

Supervisor: Erik Lind, Co-supervisor: Peter Samuelsson

Department of Physics  
Division of Mathematical Physics  
Thesis performed at the Department of Electrical and Information Technology at LTH  
June 2021



## **Abstract**

Conductance was calculated for trapezoidal nanowires with different forms and strengths of imperfection using kwant, a quantum transport software package that uses a tight-binding model. In this thesis it is found that increasing magnitudes of different imperfections such as surface charge and roughness roughen conductance steps, introduce resonances, and lower conductance overall with different character of these effects for different types of imperfections. Quantitative qualification of the effect on conductance is calculated in the form of exponential fits for Urbach tails, showing a more gradual increase in conductance as the strength of imperfections increases. These results show how different imperfections can affect transport properties in nanowires, and provide insight which can help provide a more concrete theoretical understanding of the transport-imperfection relationship as well as aid the design and characterisation of next-generation nanowire devices.

# Contents

<b>Abstract</b>	<b>i</b>
<b>1 Introduction</b>	<b>1</b>
<b>2 Theory</b>	<b>5</b>
2.1 Tight-Binding Model - kwant . . . . .	5
2.2 Conductance for a Perfect Nanowire and Energy Scaling . . . . .	6
2.3 Describing the Effects of Imperfections - Barriers and Resonances . . . . .	7
2.3.1 Band Tails . . . . .	8
2.3.2 Urbach Tails . . . . .	8
2.4 Temperature Averaging . . . . .	8
<b>3 Method</b>	<b>10</b>
3.1 Simulating Imperfections . . . . .	10
3.1.1 Surface Roughness . . . . .	11
3.1.2 Dopant/Surface Charge . . . . .	12
<b>4 Results</b>	<b>14</b>
4.1 Surface Roughness . . . . .	14
4.2 Electric Charge . . . . .	16
4.2.1 Surface Charge . . . . .	16
4.2.2 Dopant Charge . . . . .	18
4.3 Lead-Wire Connections . . . . .	19
4.3.1 Box/Corner Connection . . . . .	19
4.3.2 Doped Connections . . . . .	20
4.4 Wide Wire . . . . .	21
4.5 Temperature Averaging . . . . .	22
<b>5 Outlook</b>	<b>24</b>
5.1 Acknowledgements . . . . .	25
<b>A More Imperfections</b>	<b>29</b>
A.1 Bunching . . . . .	29



A.2	Energy Doping . . . . .	30
A.3	Placed Dopant Runs . . . . .	31
A.4	Potential Barrier Connection . . . . .	33
A.5	The Code . . . . .	33

# 1. Introduction

Nanoscale devices such as nanowires are important parts of modern nano-technology and have been a subject of active research for the past twenty years [1]. Nanowires are small cylindrically-shaped structures with diameters of the order of tens of nanometres, long and thin enough that they can be considered quasi one-dimensional for many purposes (Fig. 1.1 below). They have been constructed in various shapes and sizes, of various materials both metallic and semiconducting. Semiconductor nanowires in particular have useful features such as high reliability that make them ideal for incorporation in nano-electronic devices like transistors, where their tiny dimensions fit the constant drive for smaller scale. Fields of potential nanowire application such as quantum computing, photonics, and nano-electronics make use of the unique properties of semiconductor nanowires, and in many of these fields the search for nanowires with more favourable properties as well as a greater understanding of their properties is ongoing [1][2].

Motivated by recent experimental observations, the aim of this project has been to develop a better understanding of the effect of various realistic imperfections on the transport properties of semiconductor nanowires. Electronic transport properties are particularly important for the characterization and application of nanowires [1]. kwant [3], an open-source software package implementation of a simple tight-binding model, is used to simulate quantum electronic transport in semiconducting nanowires. To investigate the effect of non-ideal physical imperfections such as surface roughness, impurities, lattice non-uniformity, and surface charge on the transport properties of nanowires these properties are directly simulated in the model. These imperfections are present to varying degrees in all nanowires, and lead to non-ideal effects which often must be considered [4]. Nanowires are an important emerging technology; a better understanding of their effects on transport properties could aid future interpretation of experimental measurements and inform nanowire design, and by doing so advance fields of research and lead to useful technological applications.

Semiconductor nanowires are a new material technology possessing unique characteristics which show promise for application in various fields. The wavelength-of-light size scale gives ordered arrays of nanowires unique optical properties which can be utilized in different areas of research such as photovoltaics and random lasing [2][5]. As tiny semiconductors, they could possibly be used in nano-scale transistors or plasmonic circuits [1]. Having a size-scale for which quantum mechanical effects are relevant, properties such as quantized conductance can be utilized in the design of quantum computers [1]. There are a myriad of possible uses for nanowires, from simple, scaled-down versions of larger wires to devices using the physics that emerges only in such small-

scale structures, though for many uses a fuller understanding of nanowire properties and how they can be modified is still needed.

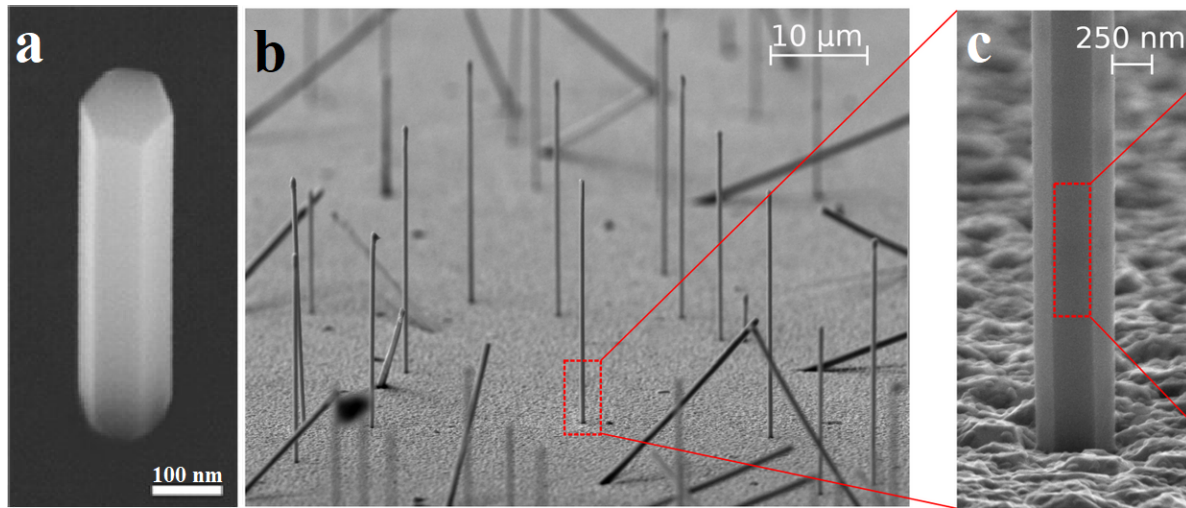


Figure 1.1: Images of (a) InGaAs/InGaP core/shell nanowire used in an array laser [6], and (b, c) ferromagnetic nanotubes [7]. The nanowire/tubes are relatively smooth with faces showing their crystalline structure, while the surface below the nanotubes is rough.

Nanowire fabrication can be a complicated process involving compromises in various properties in order to achieve various device goals – a better understanding of the effect of imperfections on a nanowire’s performance can inform such decisions. An obvious use of nanowires is in semiconductor fabrication, where nanowires would be fabricated in a complex array of other materials, with potential non-uniformities in the form of foreign atoms diffusing into a nanowire, a rough surface (Fig. 1.2 below), and surface charges, among others [8]. When designing processes for such fabrication it is sometimes possible to, for example, choose different materials – such as a nickel metallic connection versus a gold one, or choose different fabrication procedures – such as using drive-in doping versus diffusion doping. These choices even when not directly made for the nanowire itself can change the level of imperfections in a nanowire, and thus affect its performance. This motivates research into the effects of these imperfections, to better inform process and design decisions when particular properties are wanted.

The properties of nanowires constructed of different sizes or materials can be drastically different, and the possibility of developing new, interesting properties incentives research into creating new nanowires for particular purposes. In a commercial transistor switching-speed, stability, and reliability in room-temperature conditions could be paramount [1]. In some research, devices should be able to operate at a temperature five hundred degrees higher, in others they must have very precise characteristics near absolute zero. Different materials might be required in each case, and different levels of care taken in production. Arrays of evenly-spaced, uniform nanowires could provide useful optical interference effects, but growing nanowires of uniform height and thickness, or with even spacing between wires, proves challenging [2]. The design of new nanowires or more precise and reproducible fabrication methods is hoped to solve problems and fill gaps in current research; creating nanowires with superior properties is something that is hoped for to achieve

widespread practical use for nanowires in, for example, photonics and nano-electronics [1][2].

Surface charge can be accumulated in various ways; knowing its effects can help design methods and interpret measurements. When performing experiments with nanowires, one often encounters difficulties due to their small size and fragility. Often nanowires are grown en-masse, then taken and arranged on the surface of some substrate for measurements. The process by which they are collected and the substrates on which they are placed can theoretically introduce some amount of surface charge to – or deform the surface of – a nanowire. During an experiment these things can change - if charge is run through a nanowire, or the atmosphere in which the wire is placed is changed, for example, one would expect this to affect the surface charge distribution on the wire.

Conductance through nanowires can show non-ideal characteristics that could be better-explained with a fuller understanding of the relation between imperfections and transport. Surface charge, roughness, and other properties affect the conductance of a nanowire [4][9]. Theoretical calculations of density of states that consider impurity levels show band-tails and impurity bands [9]. Resonances can obscure the steps of quantized conductance, different fabrication techniques lead to different electron mobilities, and other non-ideal behaviours can be experimentally observed that are presumably caused by imperfections in measured nanowires (or measuring setups) [4]. As the properties of a nanowire that are relevant for many uses can be seen in the conductance, observations of electronic transport that show these behaviours can be more readily and positively interpreted by a more thorough understanding of the related causality.

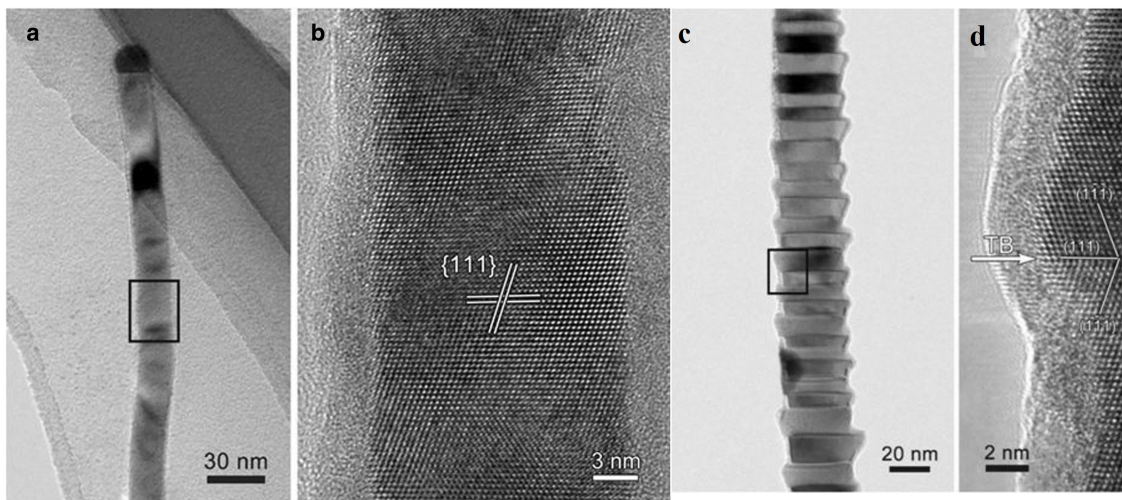


Figure 1.2: Bright-field transmission electron microscope images of (a) smooth nanowire and (c) zigzag-morphology nanowire, with high resolution images (b and d) showing the outlined sections of the bright-field images [10]. The crystal structure of the InGaAs nanowires can be seen, showing some possible different surface structures.

A relatively straightforward and simple method to probe how the transport properties of nanowires are affected by structural imperfections is to use computer simulations. In this project a tight-binding model is used to run such simulations – tight-binding models are a fairly general and simple, but effective approach to calculating electronic band-structure. In such a model, points in a lattice are simulated with an associated energy for each point as well as for hoppings be-

tween points [3]. This allows for direct simulation of surface roughness and doping/surface charge through direct control of the lattice sites and site energies respectively. By calculating the transport properties of a simulated wire for different values of roughness, doping, and perhaps other properties, a quantitative relationship between these parameters and the transport is shown. Though such a simulated model necessarily lacks much of the complications and physical nuances of a real system, the ease of creation and robust simplicity of this model make it well-suited to the task.

In this project a simple tight-binding model is developed to simulate the transport properties of nanowires with varying levels of imperfection in the form of surface roughness, charge, impurities, and others. Quantitative and qualitative relations between these imperfections and the transport properties are demonstrated. It is hoped that these findings will aid future understanding of these relations for actual nanowires and thus aid the advance of such research and technology.

## 2. Theory

### 2.1 Tight-Binding Model - kwant

To simulate nanowire properties a software package for tight-binding model computations with a focus on quantum transport was used: kwant. kwant is a Python software package for numerical quantum transport calculations, using a tight-binding model [3]. In this model a description of a physical system is built from a lattice of sites which correspond to atoms or molecules. The tight-binding lattice is created by specifying the location of sites, their energies, and site-site hopping energies. Then semi-infinite leads with the same lattice structure of the wire are attached to either end of the wire, and kwant performs a quantum transport calculation at some energy from which conductance data is retrieved to build up a conductance spectrum.

Tight-binding models are discrete models that can be used to describe a vast variety of systems and phenomena in quantum physics. Such models can be fairly simple to make and represent a variety of systems, making them a good choice to represent the general case of a semiconductor nanowire. The systems considered here are comprised of a finite scattering region (the lattice) with a few semi-infinite electrodes (the leads) connected to it. The scattering region is a lattice described by the three-dimensional Schrödinger equation (Eqn. 2.1):

$$H = \frac{-\hbar^2}{2m} (\partial_x^2 + \partial_y^2 + \partial_z^2) + V(x, y, z) \quad (2.1)$$

with hard-wall confinement outside of the wire in the x- and y-directions [3]. To be able to implement this continuous Hamiltonian as a tight-binding model in kwant, it must be discretized. To do this, each lattice site is represented by integer coordinates in a square lattice  $(i, j, k)$ , with real-space coordinates  $(ai, aj, ak)$  for some lattice constant  $a$ . The second-order derivatives can then be expressed in the limit  $a \rightarrow 0$  as:

$$\partial_x^2 = \frac{1}{a^2} \sum_{i,j,k} (|i+1, j, k\rangle \langle i, j, k| + |i, j, k\rangle \langle i+1, j, k| - 2|i, j, k\rangle \langle i, j, k|) \quad (2.2)$$

with equivalent expressions for  $\partial_y^2$  and  $\partial_z^2$ . This discretized Hamiltonian approximates the continuous one well for all quantum states with a wavelength considerably larger than  $a$ .

The transport properties are calculated using the wave function formulation of the scattering problem. With the Hamiltonian built up as described above (with the addition of the leads), propagating modes are built up as a sum of outgoing, incoming, and scattering wave functions. Matching

the wave functions in the leads with that in the scattering region gives the result: the scattering matrix. Conductance data is then simply obtained from the scattering matrix.

## 2.2 Conductance for a Perfect Nanowire and Energy Scaling

The expected form of the conductance-energy curve for a nanowire without any imperfections can be found by considering the allowed energy-states for electrons within a nanowire. The conductance should be proportional to the number of allowed states within the wire. If the nanowire has a rectangular cross-section, the electrons are bound in two dimensions and this is equivalent to the sum of energy-allowed states in a two-dimensional quantum well, for which the energy of each state is:

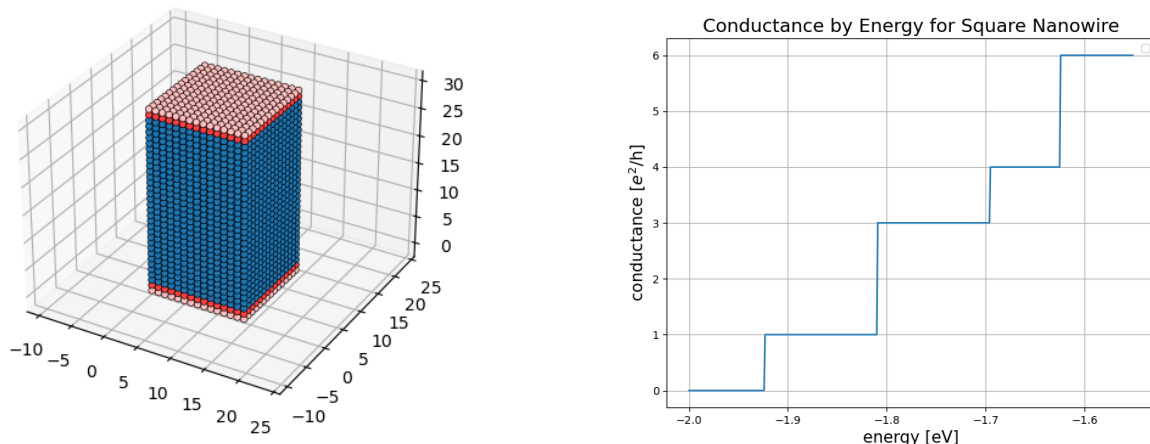
$$E_{n_x, n_y} = \frac{\hbar^2 \pi^2}{2m^*} \left( \frac{n_x^2}{l_x^2} + \frac{n_y^2}{l_y^2} \right) \quad (2.3)$$

where  $l_x$  and  $l_y$  are the x and y side-lengths, respectively, and  $n_x, n_y \in \mathbb{N}$ :

Since the units used in the simulation are chosen to be as simple as possible for ease of calculation, a step of unit-conversion needed to be made after simulations to plot in more intuitive units. Using the default units for kwant, the unit of energy in the simulation is  $t = \frac{\hbar^2}{2m^*a^2}$  and  $a = 1$  nm is the unit of distance. Using eV as the unit of energy for calculations, conversion from units of  $t$  to eV involves multiplication with a factor of (using an effective mass for InGaAs of  $m^* = 0.03 m_e$ ):

$$E(\text{eV}) = E(\text{J})/e = E(t) \cdot \frac{\hbar^2}{2m^*a^2} \text{ J} \cdot \frac{1}{(10^{-9} \text{ m})^2} \cdot \frac{1}{e} = E(t) \cdot 1.27 \frac{\text{eV}}{t} \quad (2.4)$$

To confirm that the energy-scale used for calculations with the simulation is correct, a quantitative comparison between a calculated property of the simulated nanowire and the predictions of a simple, continuous theoretical model was made. Here the sub-band spacing energies of the first few steps in conductance are compared with the simple, theoretical formula for an infinite quantum-well. To do this a long square nanowire was simulated, and the energies of the first few steps in conductance were calculated. These were compared with the formula for energy-levels of an infinite square quantum-well, which are given by Eqn. (2.3). Since there is no convenient 'zero energy' for 3D nanowires to compare with, the 'subband spacing' between two jumps in conductance is compared with the difference in energy between levels of the theoretical infinite well. For clarity, below is an image of the simulated nanowire alongside its calculated conductance plot (Fig. 2.1):



(a) Plot of nanowire, sites represented as blue spheres (wire) or red spheres (lead).

(b) Conductance plot for a 15 nm by 15 nm square nanowire, calculated using kwant.

Figure 2.1: a) Image of simulated square nanowire. b) Conductance plot for the same nanowire, showing quantized conductance steps.

Due to the difference between the continuum nature of the infinite-well theory and the finite nature of the nanowire simulation, it is expected to find an energy difference between the simulation and theoretical calculation that decreases as the quantization size decreases, or (equivalently) the system size increases. The effect of this is that the first few energy levels of the simulation are lower by a small factor; these factors are tabulated below for the interested reader, using a lattice constant of  $a = 1$  nm and energy values for the third conductance step:

Wire cross-section	5x5	10x10	15x15	20x20
$E_{theor}/E_{sim}$	1.37	1.25	1.15	1.12

Table 2.1: Conductance-step energy-difference factors between theoretical calculation and simulation, for square nanowires of different dimensions.

### 2.3 Describing the Effects of Imperfections - Barriers and Resonances

The tight-binding model used to simulate nanowire structures and calculate conductance is a quantum mechanical model - to describe the way that imperfections affect the conductance the language of barriers and resonances is used. Resonances take the form of sharp, energy-localized decreases in the conductance data, occurring centred around energies where reflection of the electrons happens. These sharp bumps can obscure conductance steps and are a feature of even experiments that take steps to avoid them [14].

Many imperfections have effects that can be broadly categorized as disorder effects - essentially the introduction of random scatterers such as impurities from doping, which can smooth out the step function of allowed states [15][16]. This disorder effect can be seen as a broadening of conductance steps, oscillatory behaviour in the steps, and suppression of the magnitude of conductance.



### 2.3.1 Band Tails

Imperfections of various types such as disorder from random scatterers interrupts otherwise sharp band edges leads to band tails. In the ideal case of a simple, perfect nanowire with zero temperature the conductance is a step function, with infinitely sharp step edges. As imperfections are introduced and a nanowire is altered from the ideal case, the density of states for electrons extends from a step function, gaining a 'tail' at energies preceding the first step [17][18]. This effect can be seen in conductance-energy curves and ranges in strength from slightly shifting conductance steps to higher energies while giving them a small tail to completely obscuring the steps at high levels of imperfections.

### 2.3.2 Urbach Tails

To obtain a quantitative measure of the effects of imperfections on conductance, the sharpness of the first conductance step is considered for different imperfections - the Urbach tail. This refers to the exponential behaviour seen in the tail at the edge of the first conductance step. This is typically calculated for the absorption coefficient at an optical absorption edge, but a similar figure can be calculated using a  $\log(I) - V$  plot [19][20]. This exponential I-V behaviour can be written in the following simple form:

$$I = I_0 e^{UV} \quad (2.5)$$

where  $I_0$  is the prefactor and  $U$  the exponential factor which characterises the sharpness of the tail. This exponential factor is expected to be larger for nanowires with lesser imperfections and sharper conductance steps, and so is a way of characterising the effect of imperfections.

Urbach tail fitting was performed by first calculating the current-voltage curve from the conductance data. This was done by simple integration [21]:

$$I = \frac{1}{e} \int_{\mu_1}^{\mu_2} G(E') dE' \quad (2.6)$$

where the limits of integration range from an energy at which conductance is zero to the desired voltage. Then the logarithm of the current and of Eqn. 2.5 is taken to reduce the range of magnitudes of relevant quantities. Taking the range of energies over the first conductance step where this curve was relatively flat, a least-squares method was used to find the best fit for  $I_0$  and  $U$  (see sections 4.1, 4.2.1). This could not be done for all curves, such as those with insufficient imperfections to have a tail or especially non-smooth curves that lack a clear flat region.

## 2.4 Temperature Averaging

Considering temperature insofar as it affects the Fermi function, temperatures greater than zero cause the conductance to be averaged over nearby energy values according to the temperature dependence of the Fermi function. Since this enters in the form of an exponential ( $e^{E/kT}$ ), the temperature is expected to have a negligible effect if the conductance is not varying in the energy

range of  $kT$ . This effect on conductance can be approximated, starting from the equation for conductance  $G$  as a function of transmission  $\mathcal{T}$  from Datta [21]:

$$G(E, T) = \frac{2e^2}{h} \int \mathcal{T}(E) \left( -\frac{\partial f_0(E, T)}{\partial E} \right) dE \quad (2.7)$$

where  $\frac{\partial f_0(E, T)}{\partial E}$  is the derivative of the Fermi function which can be expressed as:

$$-\frac{\partial f_0(E, T)}{\partial E} = \frac{1}{4} \beta \operatorname{sech}^2 \left( \frac{\beta(E - E_F)}{2} \right) \quad (2.8)$$

where  $\beta = \frac{1}{kT}$ . At zero temperature, this derivative becomes a delta function and the conductance  $G(E, 0)$  is simply proportional to the transmission  $\mathcal{T}(E)$ . This is the value that kwant returns when calculating conductance - to perform the integration of Eqn. (2.7) at some non-zero temperature the approximation  $\mathcal{T}(E) \approx G(E, 0) \frac{h}{2e^2}$  is made, then numerical integration is performed to find the conductance at some non-zero temperature. In a real system the transmission is a function of temperature due to changing carrier concentrations and other effects, but some of the character of temperature effects can be shown using this approximation.

## 3. Method

While the lattice used is a fairly general representation of a semiconductor nanowire, some choices were made to make the lattice closer to that of a specific material in order to compare its predictions with experimental data. The material chosen for this is InGaAs, a III-V compound sometimes used in the creation of nanowires [8]. The lattice created to represent the nanowire has a trapezoidal cross-section with an inner angle of 53 degrees, as seen in some measurements [4]. During calculations an electron effective mass for InGaAs of  $m^* = 0.03m_e$  was used.

As this model is a simple one, designed to easily and straightforwardly simulate imperfections, it does not try to exactly or rigorously simulate any particular material, or device. So, rather than try to match any complicated physical model, liberties have to be taken to simplify physical concepts such as screening length, and charge distributions.

Each simulation consisted of two major steps: the creation of the system, then the calculation step. Systems were created by first defining each site using placeholder energy values, then simulating any imperfections on this default lattice, attaching the leads, and finally calculating the energies associated with each site and site-site hopping. The conductance data was then calculated using kwant's built-in solver, which uses the wave function formulation of the scattering problem [3]. The data was then saved, and any analysis was performed on it.

These simulations were performed using an Intel i7-8700k CPU @ 3.70GHz, with 32.0GB of RAM. Simulations for the wire with 13020 sites took an average of approximately 3 hours for a run with conductance data at 2400 energy values. Simulations for the wide wire with 30825 sites, which was near the maximum system size permitted by memory limits, took an average of approximately 12 hours for a run with conductance data at 500 energy values. The vast majority of the simulation time was in calculating the conductance; the calculation step scales less well with system size than does defining the system [3]. The code used for these simulations and analyses was written in Python; it is available in a supplementary file (linked in A.5) for those interested.

### 3.1 Simulating Imperfections

To simulate imperfections in the nanowire, use was made of three properties of the tight-binding model: direct control over the sites in the model, control over the on-site energies, and control over the site-to-site hopping energies. Although some imperfections such as surface roughness and charge can be more-easily simulated using these properties than others, an attempt was made to approximate the effects of other imperfections with less-obvious analogues in a tight-binding model, such as the non-smooth 'clumping' of different atoms in the lattice. Some of these perhaps

less-realistic simulations are shown in appendix A.

Although a lattice with one cross-section that remains the same throughout its length and into the leads can be made with any length, since the leads are semi-infinite, the introduction of roughness, charges, and other irregularities necessitates that the wire be long enough for these effects to take effect. Nanowire lengths were chosen to be near 100 nm for this reason, and due to computational concerns.

Since the size of the lattice is on the order of thousands/tens of thousands of sites, large enough that they can be fairly accurately described statistically, the number and distribution of sites chosen in these processes produces substantially similar, though noticeably different, results when run multiple times for the same parameters. One should keep in mind that a slight change in the lattice can produce different resonances and other phenomena which can significantly affect the transport calculation. The code used for the simulations and their analyses is provided online for the interested reader (A.5), as its length prohibits placing it directly in an appendix.

### 3.1.1 Surface Roughness

Surface roughness is implemented by selecting a list of sites (or prospective sites) in and adjacent to the surface of the lattice, then removing (or adding) the listed sites. Selection is made by iterating over each surface site, excluding those sites in the face to which the lead will be attached, then randomly deciding whether to choose the site or not. In an attempt to create somewhat smooth roughness (as in Fig. 1.2), if the site is selected adjacent sites can also be chosen, with an exponentially decreasing probability as the level of adjacency increases. This iteration is done twice, once to remove sites from the system then once after to add new sites. When adding new sites, the iteration is over original surface sites only and the considered site(s) are those adjacent. Chosen sites are then removed/added. The chance to choose a considered site is controlled by a 'roughness' parameter – the probability to choose scaling exponentially with this parameter. Roughness is always added to a new, default lattice in order to prevent exceedingly deep changes. Because of this, the distribution of 'added roughness' to the lattice is different for each run of the simulation.

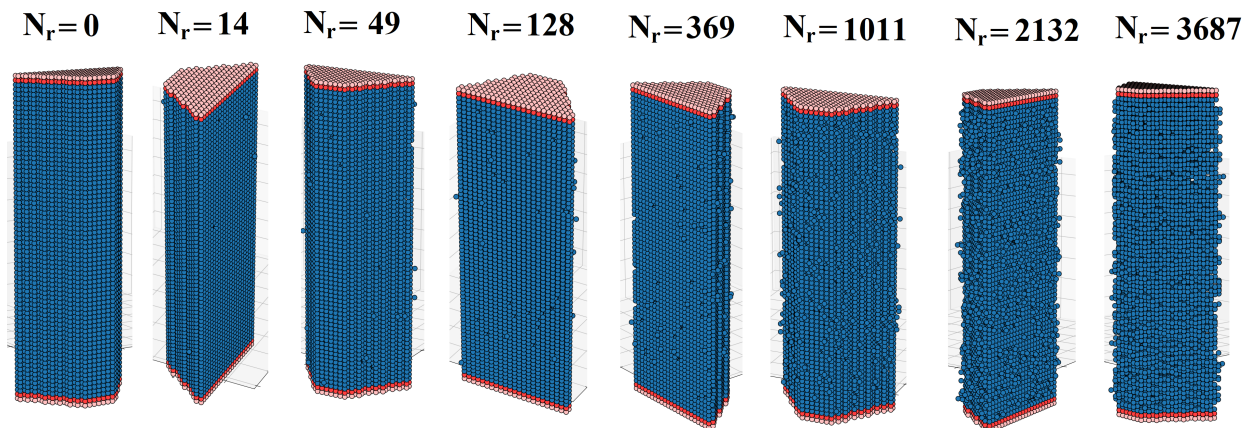


Figure 3.1: Plot of nanowire lattice, showing increasing surface roughness going from left to right, with number of altered sites  $N_r$  shown above each wire.

### 3.1.2 Dopant/Surface Charge

There were two main types of charge simulated: dopant charge, and surface charge. Charges were either dopant charges added on-site (the charged site not affected by its own charge) or surface charges added directly off-site from the surface of the wire, displaced one lattice constant away.

Surface charges were added in a similar way to roughness; surface sites are iterated over to find every adjacent empty site that have only one or two neighbouring sites in the lattice. These sites are then given a random charge according to the following formula:

$$Q = q(4r - 2) \quad (3.1)$$

where  $r$  is a random number between zero and one, and  $q$  is the average surface charge corresponding to the surface area of one site. Dopant charges were simply selected randomly from a list of every site in the wire.

The potential energy is then calculated for each lattice site using the screened Yukawa potential (Eqn. 3.2):

$$V(r) = \frac{Qq}{4\pi\epsilon_0 r} e^{-r/\lambda_s} \quad (3.2)$$

where  $\lambda_s$  is the screening length. In reality  $\lambda_s$  is dependant on material choice, carrier concentrations, and other parameters, but a simple, static choice was made for the simulation in the interest of simplicity and due to the generality of the simulated lattice. Other works show that it should be on the order of nanometres [22][23][24]. So, to determine a value of  $\lambda_s$  to best simulate the example of an InGaAs nanowire, a series of conductance curves were calculated for different values of  $\lambda_s$  (Fig. 3.2). By then comparing to the form of the conductance curve (visibility and smoothness of conductance steps) that is expected based on experimental data obtained for a previous paper [11], a value was chosen of  $\lambda_s = 1$  nm.

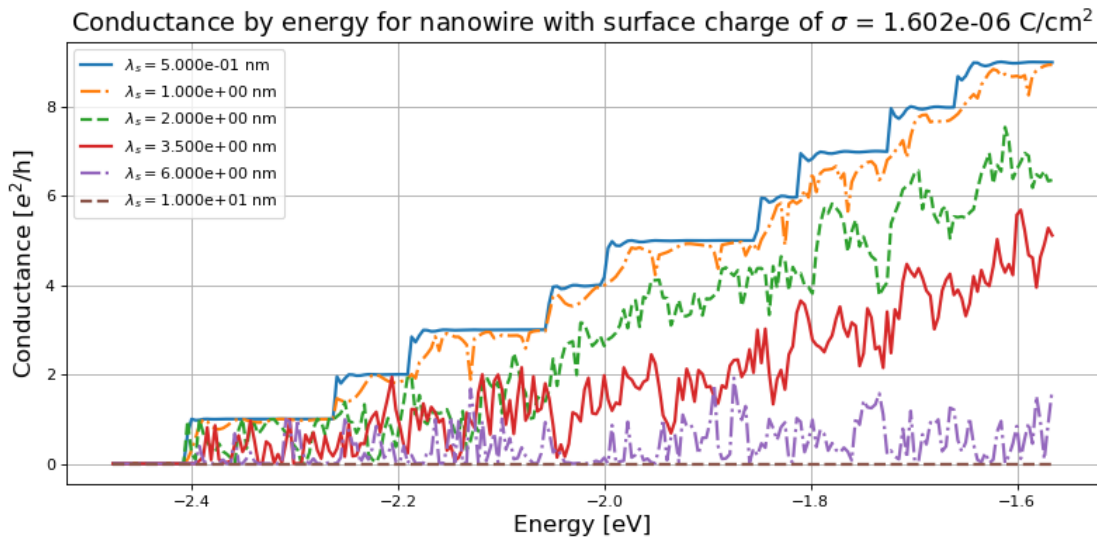


Figure 3.2: Plots of conductance by energy for a nanowire with surface charge, plotted for different values of screening length  $\lambda_s$ . At higher screening lengths, conductance shows greater deviations from an uncharged wire with more and stronger resonances as  $\lambda_s$  increases.

During calculations the potential energy for each site is multiplied by a factor to simulate different average surface charges – thus the charge distribution does not change for different values of average surface charge during a series of calculations.

## 4. Results

Results are shown for a moderately small nanowire with a lattice constant of 1 nm and corresponding dimensions of  $l = 70$  nm,  $w = 24$  nm, and  $t = 12$  nm with different surface roughness/charge and doping levels. This nanowire lattice consists of 13020 sites, 3772 of which are surface sites (images in Fig. 3.1). Then there is conductance data for alternate lead-wire connections intended to replicate a more realistic geometry, for a very wide wire such as might be used for quantum-well behaviour, and finally a demonstration of temperature effects. Runs of the simulation for various different imperfections were performed, with some of the less clear or physically justifiable simulations shown in appendix A.

### 4.1 Surface Roughness

Simulation runs for different values of surface roughness are plotted below (Fig. 4.1), showing that the conductance is noticeably affected with just a few sites changed. As  $N_r$  exceeds 14, the conductance steps become less visible as the steps become dominated by the random bumps of resonances. For values of  $N_r$  greater than about 100 the conductance steps become almost totally obscured, and the conductance is decreased overall.

The mechanism behind the effect on conductance can be explained in terms of scattering from barriers and resonances. As the structure of the nanowire becomes altered from the pristine lattice with a static cross-section, the periodic movement of electrons through the lattice can become interrupted. A missing site on the edge of the wire presents a barrier where electrons cannot propagate, or from which they must scatter. Similarly, if two sections of altered sites are spaced along a nanowire with a periodicity corresponding to the wavefunction of an electron with some energy, there could be a resonance which could result in some reflection, decreasing the transmission through the wire and so the conductance.

The location of the altered sites (which is random for each run) affects both the character and magnitude of their effect on the conductance. This can be seen by comparing the  $N_r = 7$  run (green dashed line) with the  $N_r = 14$  run (red line). The  $N_r = 7$  run shows stronger resonances and overall lower conductance compared to the  $N_r = 14$  run, which has twice the number of altered sites. This is perhaps due to strong resonances caused by specific altered sites being set up, leading to increased reflection and so lowered conductance at different energies.

A direct comparison of the roughnesses simulated here to those of real nanowires is difficult due to the loosely-correlated simulation method and non-realistic lattice used, in addition to the flat-image surface profiling method of quantifying surface roughness in real nanowires [12]. Real

nanowires can have a wide variety of surface roughnesses, with one example showing root-mean-square surface roughness in a range of about 1-5 nm with correlation-lengths of about 5-15 nm [12], and other examples having roughnesses of the same order of magnitude [4][10][13]. Corresponding surface roughnesses simulated here are for  $N_r$  in the range of tens to thousands of sites changed - with corresponding conductance curves showing steps that go from clear with slightly non-ideal behaviour to completely obscured, with overall conductance severely lowered (Figs 3.1, 4.1). From this it seems that only particularly smooth nanowires will exhibit clear quantized conductance properties - smoother than many types of nanowires, though it should be noted that some of the nanowires examined here to investigate surface roughness were not created for their conductance properties.

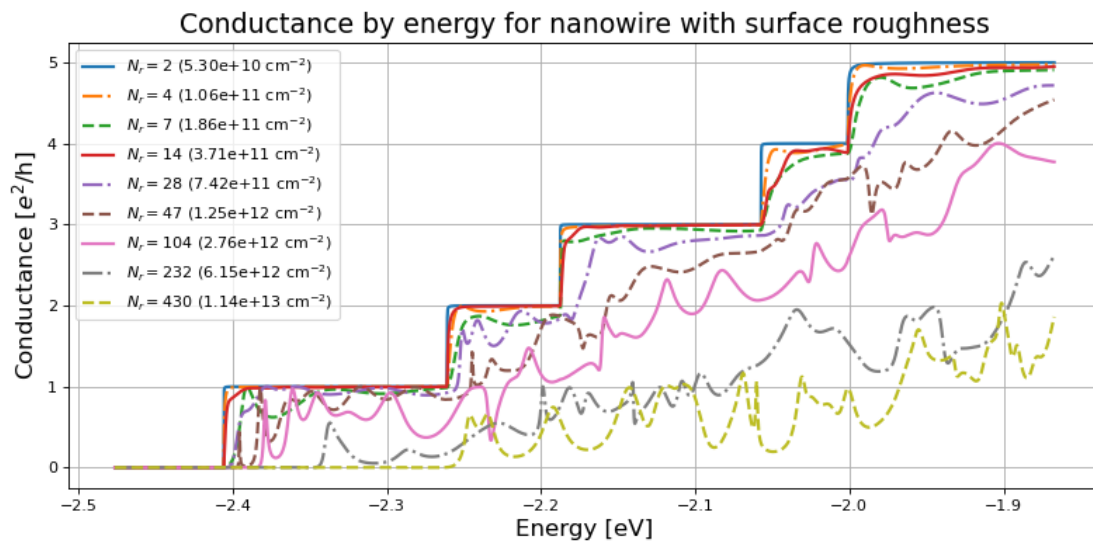


Figure 4.1: Plot of conductance by energy for nanowires with increasing surface roughness, showing increasingly obfuscated conductance steps as the roughness increases.  $N_r$  is the number of sites added and removed from the surface of the nanowire, with the corresponding surface roughness density in altered sites per square cm shown in brackets.

The logarithm of current for the runs in Fig. 4.1 was calculated, and plotted along with Urbach tail fits in Fig. 4.2. Particularly for the rougher nanowires, the spiky resonance-like behaviour causes bumps in the logarithmic curve, but fitting was performed nonetheless. As the roughness of the nanowire increases, the Urbach tail shows a generally decreasing exponential factor as can be seen in Table 4.1, giving a quantitative indicator of the effect of roughness. Urbach tails were only fitted to curves with sufficient surface roughness to affect the current noticeably.



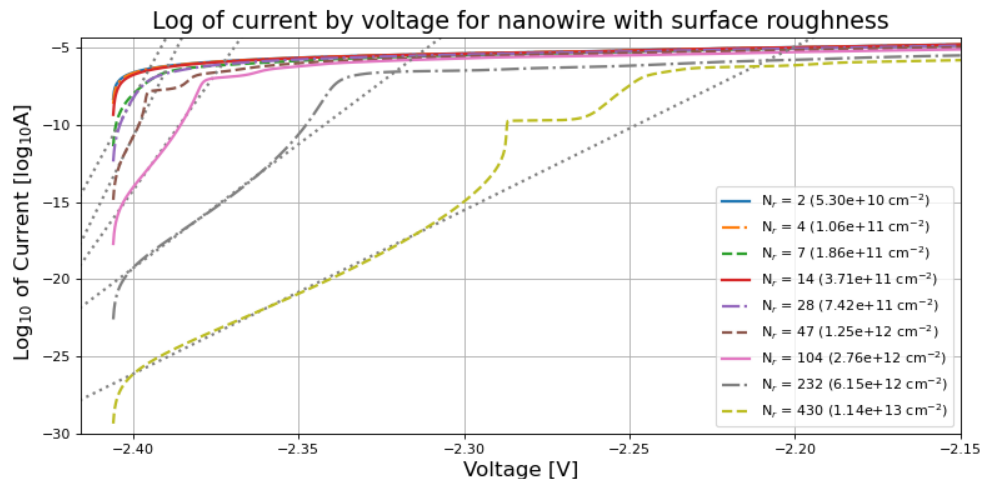


Figure 4.2: Plot of the logarithm of current by voltage for nanowires with increasing surface roughness. Urbach-tail fits are shown as dotted lines, showing decreasing steepness as surface roughness increases.

Table 4.1: Urbach-tail fit parameters for nanowire with differing surface roughness densities  $\sigma_r$ .

Surface roughness $\sigma_r$ ( $\text{cm}^{-2}$ )	$7.42 \times 10^{11}$	$1.25 \times 10^{12}$	$2.76 \times 10^{12}$	$6.15 \times 10^{12}$	$1.14 \times 10^{13}$
Inverse Exponential factor $1/U$ (mV)	1.10	1.00	1.43	2.70	4.09

## 4.2 Electric Charge

Electric charge, in the form of dopants or surface charge, is a relevant consideration in the performance of nanowires as it will always be present to some degree. The conductance of nanowires can be so affected by surface charges that they have found use as sensors by utilizing this property [1].

### 4.2.1 Surface Charge

Surface charge is represented here as charge placed one lattice constant (1 nm) away from the surface of the nanowire, distributed randomly. Simulation runs for different values of random surface charge density are plotted below (Fig. 4.3), showing conductance steps that remain distinctly visible as  $\sigma$  increases, with growing sinusoidal behaviour and steps that are shifted to increasingly higher energies. The effect is very similar to that of positive-only charge (Fig. 4.5a), where the onset of each conductance step remains sharp with oscillations beginning at the start of each step, damping as energy increases.

The mechanism behind the effect of charges on conductance is similar to that of surface roughness, where sites are entirely removed or added with identical energies to the rest of the wire. Charge effects only alter the energies of sites, making them more or less favourable for an electron travelling through the wire. Thus scattering and resonances occur, more evenly spread throughout the wire rather than present only on the surface.

A reasonable real-world value for surface charge concentration is on the order of  $6 \times 10^{-6} \text{ C/cm}^2$ , corresponding to a little less than the pink curves in the figures below. At this value the

conductance is noticeably affected, though even for the negative-only charge run the conductance steps are still visible (and would likely be more visible if temperature averaging was considered). Based on this, surface charge does seem like a reasonable consideration as higher surface charge concentrations could non-negligibly affect the conductance.

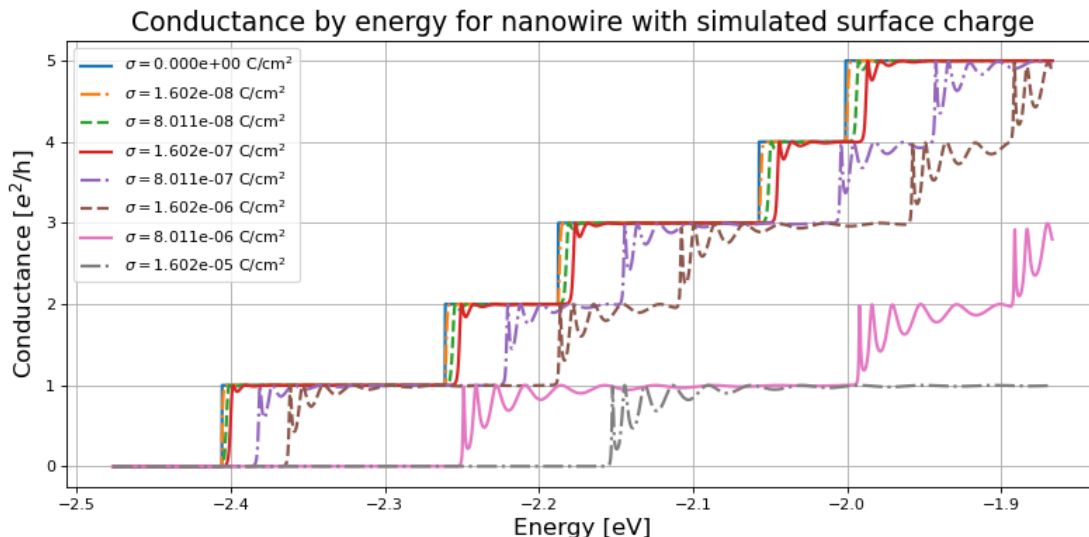


Figure 4.3: Plot of conductance by energy for a nanowire with increasing random surface charge, showing conductance steps with increasingly oscillatory behaviour and at increasingly higher energy as the charge density increases.

The logarithm of current for the runs in Fig. 4.3 was calculated, and plotted along with Urbach tail fits in Fig. 4.4. As increasing random surface charge gives a rather smooth and continuous change in conductance, the Urbach tail shows a smoothly decreasing exponential factor as can be seen in Table 4.2. Urbach tails were only fitted to curves with sufficient charge to affect the conductance.

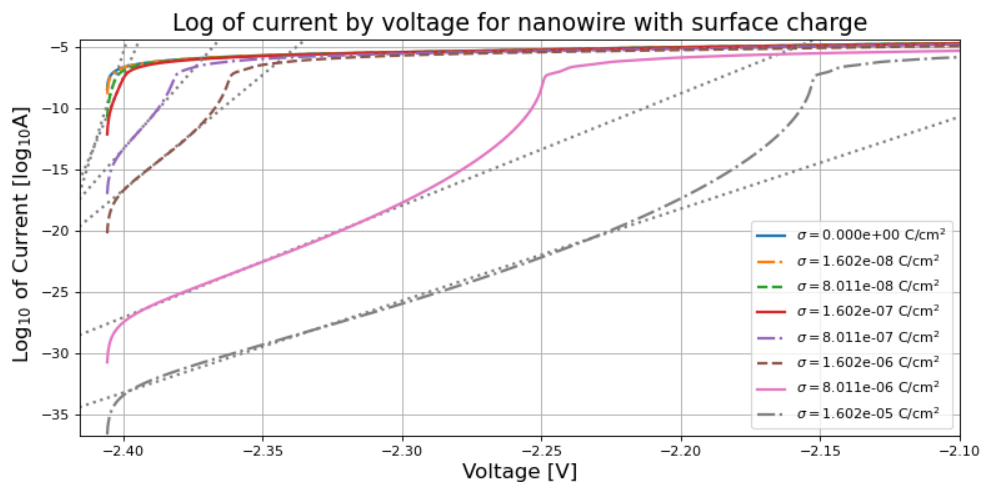


Figure 4.4: Plot of the logarithm of current by voltage for a nanowire with increasing random surface charge. Urbach-tail fits are shown as dotted lines, showing decreasing steepness as the charge density increases.

Table 4.2: Urbach-tail fit parameters for nanowire with differing surface charge densities  $\sigma$ .

Surface charge $\sigma$ ( $\text{cm}^{-2}$ )	$8.01 \times 10^{-8}$	$1.60 \times 10^{-7}$	$8.01 \times 10^{-7}$	$1.60 \times 10^{-6}$	$8.01 \times 10^{-6}$	$1.60 \times 10^{-5}$
Inverse Exponential factor $1/U$ (mV)	0.59	0.81	1.67	2.30	4.74	5.78

Simulations were also run using surface charge generated to be strictly positive or negative, in order to characterise the effect of different types of charge (Fig. 4.5). The effect of purely positive charge is very similar to that of random charge, with conductance steps shifting to higher energy, becoming wider, and gaining oscillatory behaviour with oscillations damping further along each conductance step. The lack of a sharp increase in conductance at some steps (e.g. the pink curve after -2.3 eV) is due to the large energy-step used when calculating conductance. However, the runs with negative charge show none of this behaviour and instead are dominated by very spiky resonances, following the conductance steps in energy but with decreasing conductance as the charge increases.

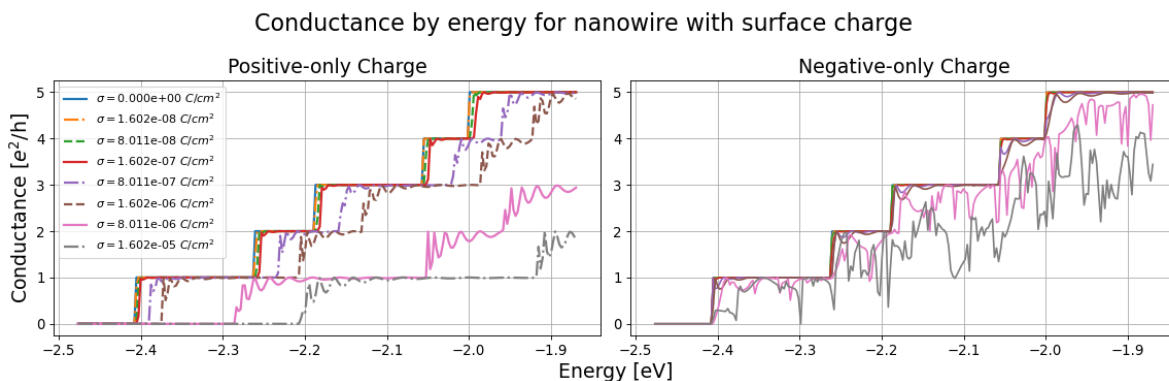


Figure 4.5: Plots of conductance by energy for a nanowire with increasing positive (left) and negative (right) surface charge, with a shared legend on the left. The runs with positive-only charge show increasing oscillatory behaviour and energy-shifted conductance steps, while the runs with negative-only charge show increasing resonances and generally decreasing conductance as charge increases.

## 4.2.2 Dopant Charge

Dopant charges here were modelled as charges with a magnitude of one elementary charge placed on semi-randomly selected lattice sites. These runs are plotted in Fig. 4.6, and show increasing disorder behaviour with more resonances as the number of dopants is increased. The runs with positive dopant charges shift the conductance steps to higher energies, while the runs with negative charges show stronger resonances.

As nanowires are small and cannot be evenly doped due to the high concentrations required for even 11 dopants, the uneven presence of impurities or dopants will necessarily create resonances and barriers to electron transport. Realistic doping concentrations for different materials and dopants might vary from  $10^{15}$  to  $10^{21} \text{ cm}^{-3}$  - the higher end of which would significantly impact nanowire conductance. However, since one can likely avoid intentionally doping a nanowire, it seems likely that only a small concentration of incidental impurities is relevant to consider, creating an affect much like surface charge.

Some runs with other attempted methods of simulating doping are in Appendix A.2, and runs with dopant charges placed at specific distances from the surface of the nanowire are in Appendix A.3.

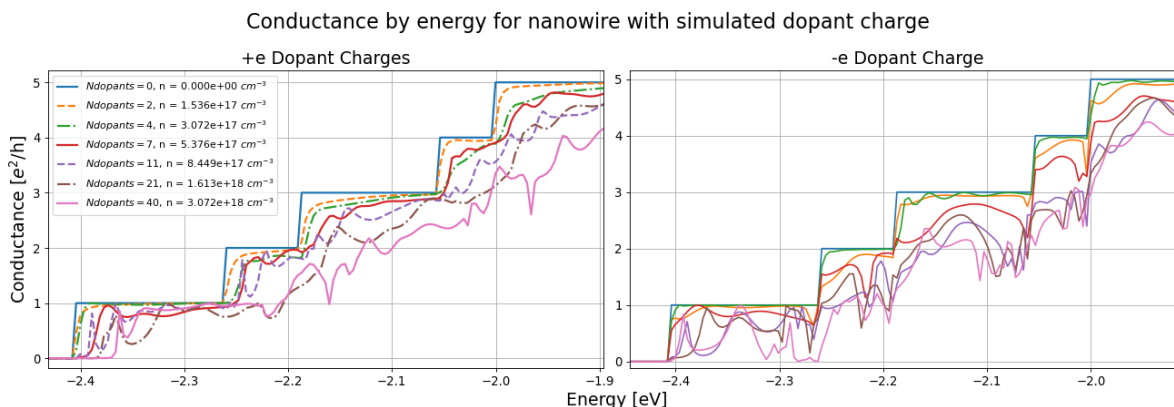


Figure 4.6: Plots of conductance by energy for a nanowire with increasing concentrations of positive (left) and negative (right) dopant charges, with a shared legend on the left. The runs with positive charge show that with increasing dopant concentration the conductance steps become smoother, shifted slightly to higher energies, and at higher concentrations the curve develop sharp, resonance-like bumps as well as generally having lower conductance. The negative-charge runs show similar behaviour with sharper resonances, except that the sharpness and energy-values of the step onsets are largely unaffected.

### 4.3 Lead-Wire Connections

The geometry of the leads' attachments to a nanowire can be a relevant consideration that affects the conductance properties. Due to the small size and fragility of nanowires, lead connections are typically much larger than the nanowire itself and are not connected in parallel with the length of a nanowire but rather inserted perpendicularly. They can also be made of different materials, differently doped, and are otherwise distinct from the nanowire itself. Considering the wave functions that are resonant within the lead, these differences present a sort of barrier to electrons as they propagate from the lead to the wire and vice versa – to investigate this effect, simulations were run for nanowires with various different lead-wire connections.

It should be noted that the lead connection is larger than and often made of a different material from the nanowire itself, and so electrons can enter the regime of ballistic transport where they can travel long distances freely, rather than the scattering regime used in these simulations. The connections were not simulated any differently than the wire itself, here.

#### 4.3.1 Box/Corner Connection

As leads are typically not nanowires themselves, they are much larger than the wires they connect to. To simulate this, some runs were made with lead-connections much wider than the wire itself. The sudden thinning of the path results in a choke-point - the energy required for an electron to travel in the wire is greater than that of the lead, and resonances might be caught in the volume of the lead-wire connection as electrons scatter back and forth, reducing conductance. Lead connec-

tions are also typically made perpendicularly to the length of a nanowire - which one might expect to provide another disconnect barrier with associated resonances.

Some runs are plotted below for different types of lead-wire connections (Fig. 4.7), and in Appendix A.4. The straight rectangular connection's first five conductance steps are easily distinguishable, but later steps grow increasingly obscured by resonances. The rectangular corner connections show poorer properties, dominated by resonances and without distinguishable conductance steps. The flat-backed ovular connection has fewer and weaker resonances, similar to the straight rectangular connection - it shows the best properties of the corner connections.

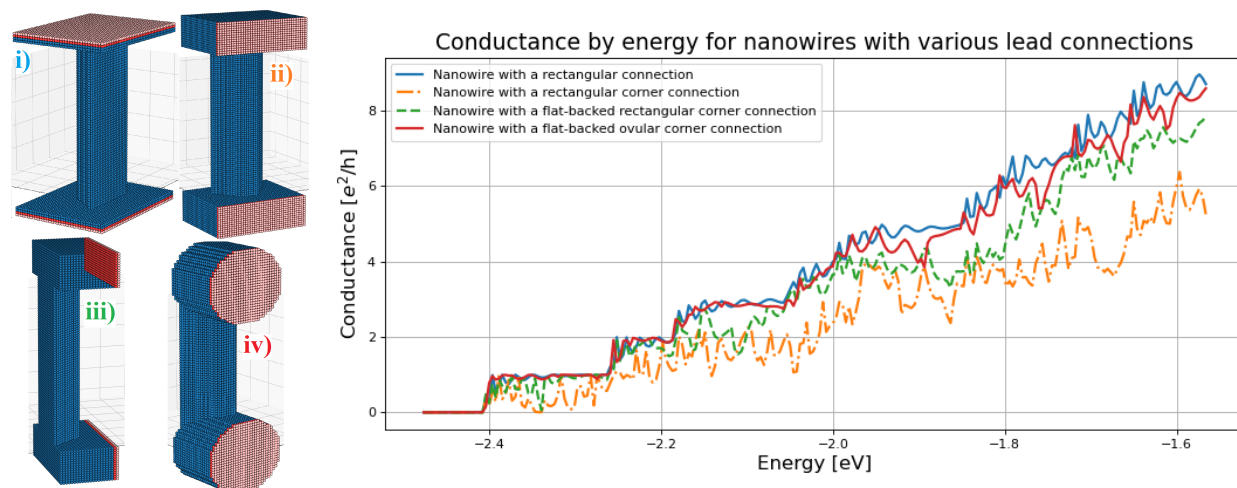


Figure 4.7: Images of different lead-nanowire connections (left) alongside a combined plot of their conductance curves (right). Different lead-wire connections (lead connection shown in red) are: **i)** Simple rectangular connection, **ii)** Rectangular corner connection, **iii)** Flat-backed rectangular corner connection, **iv)** Flat-backed ovular corner connection. All of the conductance curves show varying levels of spiky, resonance-like bumps and obscured conductance steps, especially at higher energies.

### 4.3.2 Doped Connections

Many lead-wire connections are composed of a material which is doped to make it conductive - some runs were made with a doped lead-wire connection to see how doping in this area affects the conductance. The flat-backed ovular corner connection was used to provide the greatest contrast between doped and non-doped lead connections, as the conductance steps are most distinct for that type of connection. Some runs are plotted below for different dopant concentrations 4.8. Compared to the run without dopants, increasing dopant levels introduce more resonances and at high levels the conductance is lowered overall. At extremely high dopant concentrations even the first step becomes obscured, though the conductance still follows underneath the step pattern to some degree.

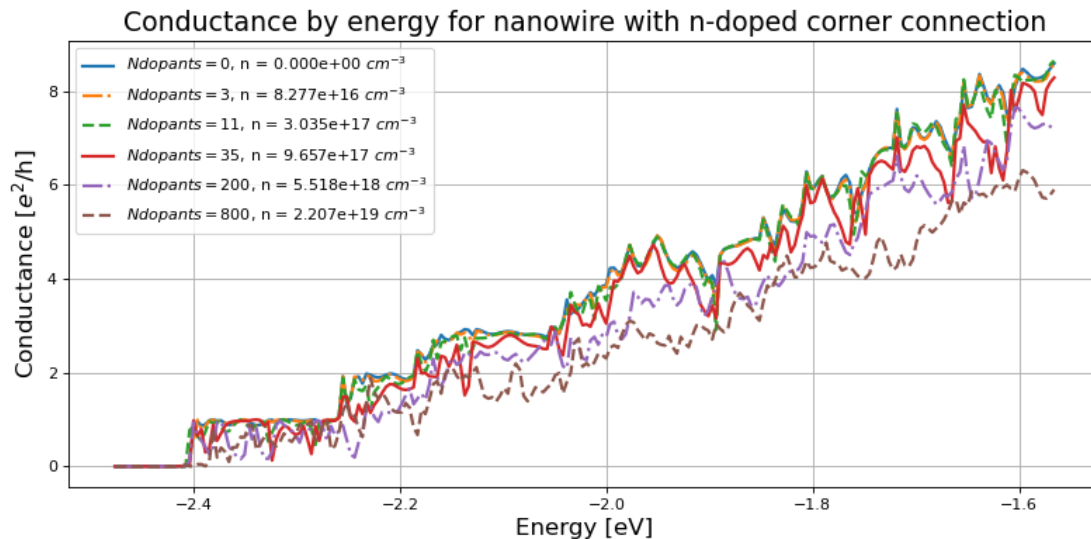


Figure 4.8: Plot of conductance by energy for a nanowire with a negatively doped ovular flat-backed lead-wire connection (see Fig. 4.7 iv). Lower concentrations of dopants show a similar pattern of resonances to the un-doped nanowire, and do not further obscure the conductance steps. Higher concentrations of dopants intensify the noisy pattern of resonances, reducing the conductance overall as well as obscuring the steps.

#### 4.4 Wide Wire

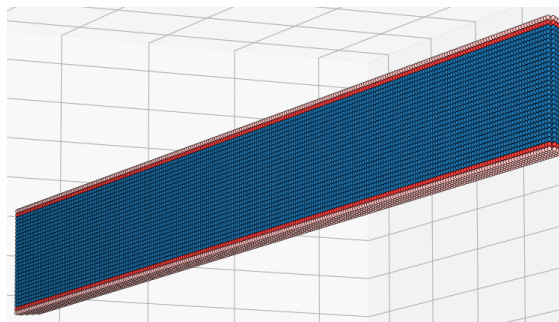


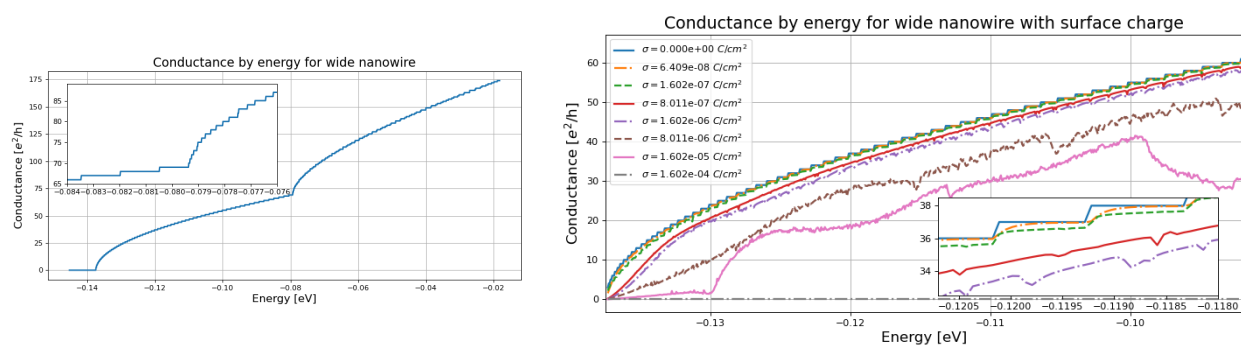
Figure 4.9: Plot of wide nanowire lattice with sites represented as blue spheres (wire) or red spheres (lead), corresponding to a nanowire with real dimensions of 20x100x1000 nm.

Some simulations were run using a very wide wire, expected to show properties similar to a quantum well (Fig. 4.9). A very wide nanowire is expected to show a 'double-step' pattern of very distinct conductance steps: wide steps of higher energy corresponding to the shorter dimension, and short steps building on those wide steps for the wide dimension of the wire. Since this requires creating a larger lattice with many tens of thousands of sites, computer memory limits and computation time become more of a concern, necessitating a larger lattice constant for the wider wire. To simulate a wire with a width of about one micron, I ran simulations analogous to those for the 'regular' nanowire using dimensions of  $l = 25$ ,  $w = 250$ , and  $t = 5$ , corresponding to a lattice constant of  $a = 4$  nm and a lattice containing 30825 sites, 13920 of which are surface sites. The double-step pattern in the conductance curve can be seen in Fig. 4.10a.



Runs with surface charge placed on the wide nanowire were also run (Fig. 4.10b). Lower concentrations of charge first obscured the smaller conductance steps and shifted the step energies up, with higher concentrations obscuring the large-scale pattern with more and larger resonances. It is worth noting that the lattice constant is 4 nm for the wide wire and the wire is only 5 sites thick, while the charges were still placed 1 nm from the surface of the wire. Because of this, the effects of the charge 'reach' farther inside the wire than would be allowed by charge screening if the lattice constant was smaller.

Surface charge concentrations on the order of  $10^{-6} C/cm^2$  obscure the smaller conductance steps, with larger concentrations leaving them totally obscured and only the larger step-pattern visible. While this could be a result of the larger lattice constant used for this wire, it also implies that wide-nanowire applications which require clarity of the smaller conductance steps could face problems with surface charge more easily than a regular nanowire.



(a) Plot of wide nanowire conductance over a large range of energies, showing double-step pattern with  $\sqrt{E - E_n}$  behaviour. Inset shows a smaller range of energies centred around the end of the first large conductance step.

(b) Plots of wide nanowire conductance with increasing random surface charge, showing conductance steps smoothed and shifted to higher energies as charge increases. At higher concentrations, resonances obscure the smaller conductance steps. Inset shows a smaller range of energies, showing the smaller conductance steps.

Figure 4.10: Plots of wide nanowire conductance over different ranges of energies, showing double-step pattern. **a)** shows a wide range of energies; **b)** shows the effect of surface charge, over a smaller range of energies.

## 4.5 Temperature Averaging

To demonstrate the effects of temperature averaging using the method described in section 2.4, two different showing the effects surface roughness and charge were analyzed and plotted below (Fig. 4.11). Since the only affect taken into account here is the changing range of electron energies described by the Fermi function, from the form of the exponential in the Fermi function the effect of this 'averaging' is expected to be essentially to average the conductance over an energy range of approximately  $kT$ . This can be seen, as at lower temperatures some spiky and quickly oscillating behaviour can be seen to be averaged out, and at higher temperatures entire conductance steps start to become broadened and smoothed out.

As changing temperature would also affect a real nanowire in other ways, such as changing carrier concentration and induced electric fields, these results should be interpreted with a grain of

salt.

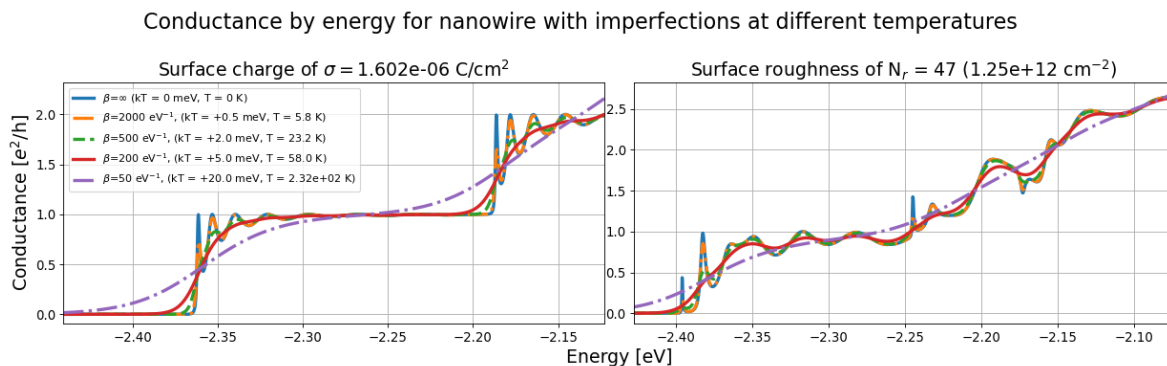


Figure 4.11: Plots of nanowire conductance at different temperatures, showing the effect of Fermi broadening leading to smoother curves at higher temperatures. Plots are shown for two different nanowires, showing visibility of the conductance steps first increase as sharp oscillations are averaged over then decrease as entire steps are averaged over as temperature increases.



## 5. Outlook

The quantum transport properties of trapezoidal nanowires with various types of imperfections was studied. By simulating quantum transport in 3-dimensional lattices representing nanowires a qualitative and somewhat quantitative relationship was assembled between various unavoidable imperfections in nanowire lattices and their engendered imperfections in the conductance spectrum. The plotted results can hopefully be of use to people interested in knowing the levels of imperfection that will affect nanowire conductance behaviour: for example the amount of surface roughness that can be tolerated before the first few quantized conductance levels become quashed.

A possible route for future work could be to investigate time-dependant behaviour, which is relevant for many applications of nanowires. The effect of dynamic charge could be of interest for the use of charge-sensing in fluids. Non-static behaviour such as on-off switching behaviour is important for nano-electronics. A version of kwant designed to tackle time-dependant problems, 'tkwant', might be used to simply extend current code for such a purpose.

More consistent data could be obtained for surface charge and roughness by averaging the conductance data over a large number of consecutive runs with the same parameters. While the data presented herein was at the limit of what could be collected on the author's personal computer, if one could afford the cost in computation time this would be a way to avoid the random nature of the resonances' effects on conductance. Many of the imperfections' effects appeared pseudo-random and were different between each run of the simulation due to the random distribution of charge and roughness along the wire. Although averaging over resonances and perhaps other oscillatory behaviour would prevent them being visible, this would give a better idea of the average level of conductance one should expect rather than the particular form one might find in one measurement.

If one was interested in relatively exact, quantitative results for a situation similar to those presented in this paper, an approach with a stricter adherence the physics of the particular situation would likely be needed. A future simulation could more accurately model the lattice of a particular material, and using that lattice model specific types of impurities or dopants, among other things. One might take into account the effect of electron orbitals, more physically model electric charge screening and electric charge quantization, among other things that were more or less ignored in the interest of simplicity and generality for this work.

A better understanding might be reached by comparing the results of these simulations with measurements, insofar as this is possible. The real, physical situation is always more complicated than what can easily be simulated, so by comparing the simulated effects of some imperfections with their experimental analogues one might achieve a better understanding of the cause of these

effects. This would also help to establish the accuracy of the simulation method used here. While surface charge and roughness might conceivably be measured directly, imperfections such as impurities and slight irregularities in a crystal lattice are typically inferred from properties such as the conductance and could not easily be compared with this simulation.

## **5.1 Acknowledgements**

This would not have been possible without the guidance of my supervisor, Eric Lind, useful advice from my co-supervisor, Peter Samuelsson, and the aid of posters on the kwant mailing list.

## Bibliography

- [1] N. P. Dasgupta, J. Sun, C. Liu, S. Brittman, S. C. Andrews, J. Lim, H. Gao, R. Yan, and P. Yang, 25th Anniversary Article: Semiconductor Nanowires – Synthesis, Characterization, and Applications, *Advanced Materials* volume 26, issue 14, pages 2137-2184 (2014); <https://doi.org/10.1002/adma.201305929>
- [2] D. Pisignano, L. Persano, and A. Camposeo, Perspectives: Nanofibers and nanowires for disordered photonics, *APL Materials* 5, 035301 (2017); <https://doi.org/10.1063/1.4974481>
- [3] C. W. Groth, M. Wimmer, A. R. Akhmerov, and X. Waintal, Kwant: a software package for quantum transport, *New J. Phys.* 16, 063065 (2014); <https://doi.org/10.1088/1367-2630/16/6/063065>
- [4] C. B. Zota, D. Lindgren, L.-E. Wernersson, and E. Lind, Quantized conduction and high mobility in selectively grown  $\text{In}_x\text{Ga}_{1-x}\text{As}$  nanowires, *ACS Nano* 2015, 9, 10, 9892–9897; <https://doi.org/10.1021/acs.nano.5b03318>
- [5] G. Tchutchulashvili, S. Chusnutdinow, W. Mech, K. P. Korona, A. Reszka, M. Sobanska, Z. R. Zytkeiwicz, W. Sadowski, GaN Nanowire Array for Charge Transfer in Hybrid GaN/P3HT:PC71BM Photovoltaic Heterostructure Fabricated on Silicon, *Materials* Vol 13, Iss 4755, p 4755 (2020); <https://doi.org/10.3390/ma13214755>
- [6] H. Kim et al, Monolithic InGaAs Nanowire Array Lasers on Silicon-on-Insulator Operating at Room Temperature, *Nano Letters* 2017, 17, 6, 3465-3470; <https://doi.org/10.1021/acs.nanolett.7b00384>
- [7] C. Back, Smooth ferromagnetic nanotubes for the investigation of domain wall motion, <https://www.groups.ph.tum.de/efs/research/domain-wall-motion/>, Accessed: 2021-05-27
- [8] C. B. Zota, E. Lind, Size-effects in indium gallium arsenide nanowire field-effect transistors, *Applied Physics Letters* 109, 063505 (2016); <https://doi.org/10.1063/1.4961109>
- [9] A. Gold, J. Serre, and A. Ghazali, Density of states in a two-dimensional electron gas: Impurity bands and band tails, *Physical Review B* 37 (9), 1988.

- [10] L. Shang, L. Song, Y. Wang, R. Cai, L. Liu, and F. Wang, Formation Mechanisms of InGaAs Nanowires Produced by a Solid-Source Two-Step Chemical Vapor Deposition, *Nanoscale Research Letters* 13, 263 (2018); <https://doi.org/10.1186/s11671-018-2685-0>
- [11] L. Södergren, N. V. Garigapati, M. Borg, and E. Lind, Mobility of near surface MOVPE grown InGaAs/InP quantum wells, *Appl. Phys. Lett.* 117, 013102 (2020); <https://doi.org/10.1063/5.0006530117>
- [12] J. Lim, K. Hippalgaonkar, S. C. Andrews, A. Majumdar, and P. Yang, Quantifying Surface Roughness Effects on Phonon Transport in Silicon Nanowires, *Nano Letters* 12, 5, 2475-2482 (2012); <https://doi.org/10.1021/nl3005868>
- [13] C-C. Chang et al, Electrical and Optical Characterization of Surface Passivation in GaAs Nanowires, *Nano Letters* 12, 9, 4484-4489 (2012); <https://doi.org/10.1021/nl301391h>
- [14] T. Loh, T. Miyamoto, Y. Kurita, F. Koyama, and K. Iga, Reduction of inelastic scattering effect by introducing strain-compensated superlattice into GaInAs/GaInP multi-quantum barriers, *Seventh International Conference on Indium Phosphide and Related Materials* (1995), <https://doi.org/10.1109/ICIPRM.1995.522157>
- [15] L. Serra and M-S. Choi, Conductance of tubular nanowires with disorder, *European Physical Journal B – Condensed Matter* 71 (1), 97-103 (2009), <https://doi.org/10.1140/epjb/e2009-00280-6>
- [16] P. V. Mieghem, Theory of band tails in heavily doped semiconductors, *Reviews of Modern Physics* 64, 755-791 (1992).
- [17] D. N. Quang and N. H. Tung, A Semiclassical Approach to the Electron Gas in Two-Dimensional Semiconductor Structures, *phys. stat. sol. (b)* 207, 111 (1998).
- [18] A. Gold, J. Serre, and A. Ghazali, Density of states in a two-dimensional electron gas: Impurity bands and band tails, *Physical Review B* 37 (9), (1988); <https://doi.org/10.1103/PhysRevB.37.4589>.
- [19] P. Sarangapani, Y. Chu, J. Charles, and T. Kubis, Non-equilibrium Green's function predictions of band tails and band gap narrowing in III-V semiconductors and nanodevices, *Physical Review Applied* 12, 044045 (2019); <https://doi.org/10.1103/PhysRevApplied.12.044045>.
- [20] T. Li and M. Dagenais, Urbach Tail in Intermediate Band InAs/GaAs Quantum Dot Solar Cells, *2014 IEEE 40th Photovoltaic Specialist Conference (PVSC)* (2014); <https://doi.org/10.1109/PVSC.2014.6924890>.
- [21] S. Datta, Chapter 2: Conductance from transmission from 'Electronic Transport in Mesoscopic Systems' (Cambridge Studies in Semiconductor Physics and Microelectronic Engineering: 3), *Cambridge University Press* (1995); <https://doi.org/10.1017/CBO9780511805776>.

- [22] A. Wolkenberg and T. Przesławski, Charge transport diagnosis by: I–V(resistivity), screening and Debye length, mean free path, Mott effect and Bohr radius in InAs,  $\text{In}_{0.53}\text{Ga}_{0.47}\text{As}$  and GaAs MBE epitaxial layers, *Applied Surface Science* 254 (2008), 6736-6741.
- [23] A. Butterfield and J. Szymanski, A Dictionary of Electronics and Electrical Engineering (5 ed.), *Oxford University Press* (2018), section on Debye length.
- [24] A. R. Bechhofer, A. Euda, A. Nipane, and J. T. Teherani, The 2D Debye length: An analytical study of weak charge screening in 2D semiconductors, *Journal of Applied Physics* 129, 024301 (2021), <https://doi.org/10.1063/5.0032541>

## A. More Imperfections

Many simulations were run with a variety of different disorder effects, site energy patterns, shape, etc., many of which are not shown in the main text for brevity and to highlight the more realistic cases of lattice imperfections. Other plots of conductance by energy showing are shown below with their descriptions for the interested reader.

### A.1 Bunching

An attempt was made to simulate the effect of having an uneven distribution of types of atoms in a compound lattice in a simple way, without considering orbital effects and other complicated physics. This lattice bunching was modelled in the follow way: each site is iterated over, having an equal random chance of being selected which is proportional to the bunching parameter. If selected, each surrounding site has is considered for selection, having a much lower probability of being selected, and so on. The effect of the selected or 'bunched' sites is that the energy value of every hopping associated with that site is multiplied by 1.2, chosen to have a small by relevant effect. This bunching process is always performed on a 'fresh' lattice which has not had bunching before - runs are plotted below (Fig. A.1).

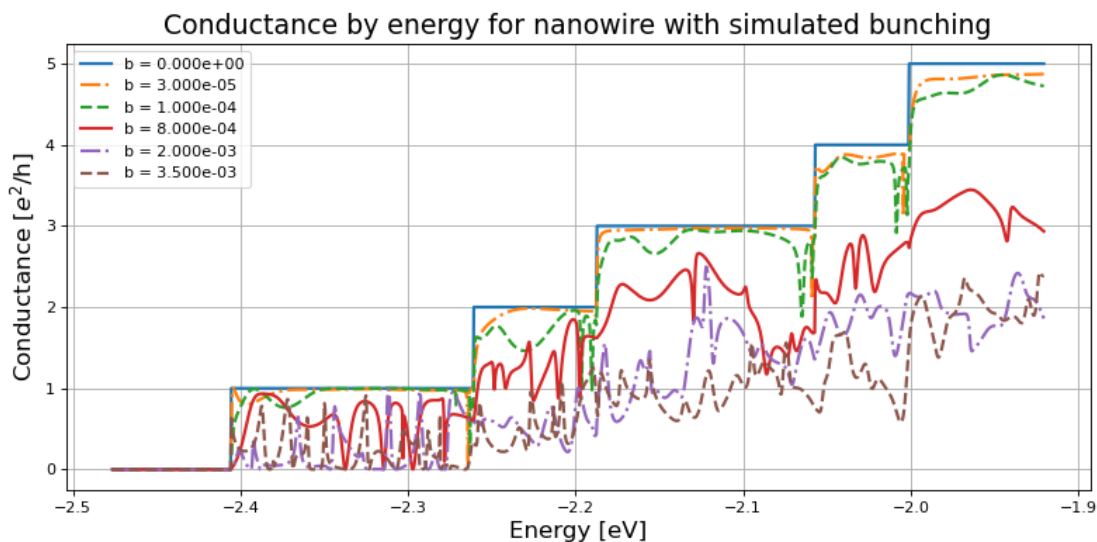


Figure A.1: Plot of conductance by energy for a nanowire with hopping energies altered to simulate 'bunching', showing increasingly obfuscated conductance steps and sharper resonances as the concentration of altered energies increases. Bunching parameter 'b' is the probability for a site to be selected for bunching.

## A.2 Energy Doping

An attempt was made to simulate the effect of dopant atoms by directly modifying site energies, rather than placing electric charges. Placed energy doping was simulated by a simple iteration over every site in the lattice, each site having an equal probability of being marked to have their on-site energy changed based on the doping concentration. The effect of doping was to alter the on-site energy by 20%, chosen to have a small but relevant effect. This selection process is repeated for each different doping concentration, possibly resulting in differing doping profiles and a different number of replaced sites for one concentration - runs plotted below (Fig. A.2).

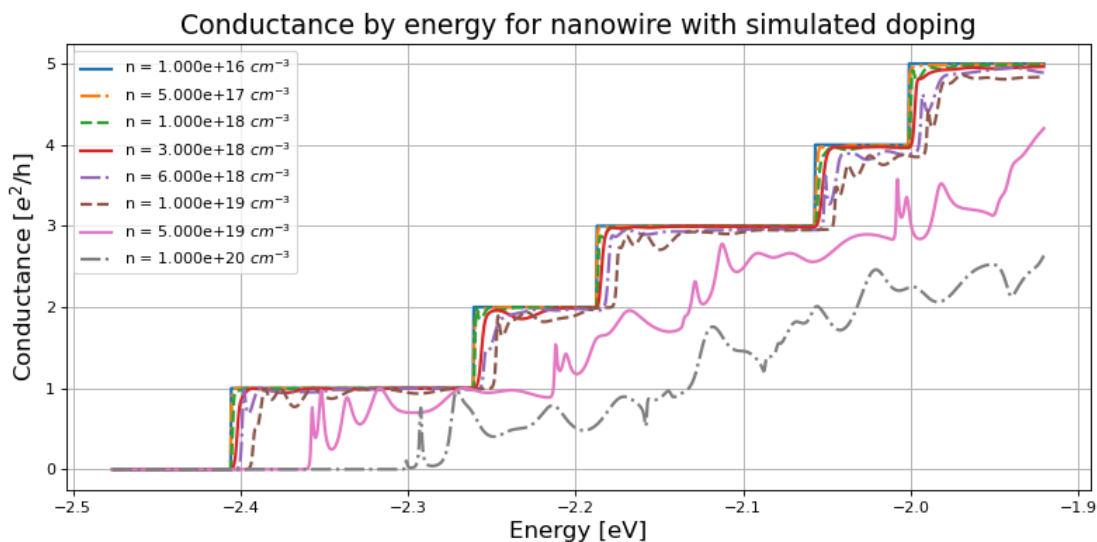


Figure A.2: Plot of conductance by energy for a nanowire with on-site energies altered to simulate doping, showing increasing energy of and increasingly obfuscated conductance steps due to resonances as the concentration of altered energies increases.

Some runs were also performed where all site energies were modified simultaneously, as a way to less-directly simulate the effect of dopants (Fig. A.3).

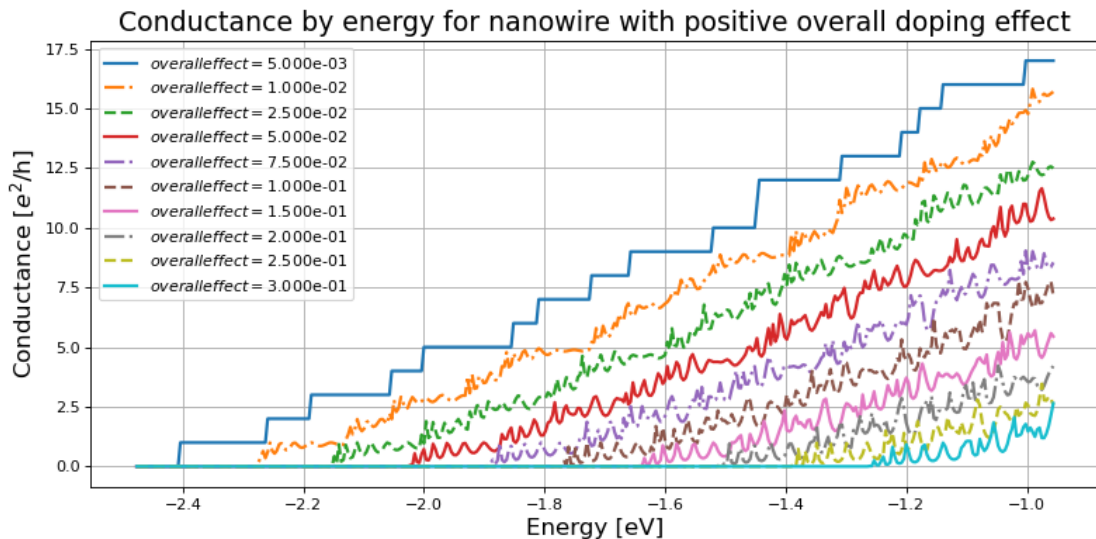


Figure A.3: Plot of conductance by energy for a nanowire with all on-site energies modified simultaneously, showing increasing energy of and increasingly obfuscated conductance steps due to resonances as the concentration of altered energies increases.

### A.3 Placed Dopant Runs

During other simulations, dopant charges were placed randomly within a nanowire, with equal probability to appear in every eligible site. It is clear that the placement of charges within the wire has a significant effect on the conductance - if one considers the case of two dopant charges placed in the centre of a nanowire so as to divide it into three equal segments, one would expect to see a resonance. Multiple runs with the same parameters will show slightly but noticeably different curves due to the different placement, some with resonances appearing at different energies, or without notable resonances at all.

So, for the interested reader below are some runs where the dopant charges were placed at certain (approximate) distances from the nanowire's surface (Fig. A.4). One should note that the charges were still placed randomly within eligible sites - they may or may not be evenly spaced throughout the wire's length and breadth. It can be seen that charges placed at or near the nanowire's surface have relatively little effect, as one might expect considering the charge-screening of the Yukawa potential. Beyond that, some runs produced the spiky, oscillatory behaviour expected of resonances while others simply had suppressed conductance - this occurring differently at different conductance steps.



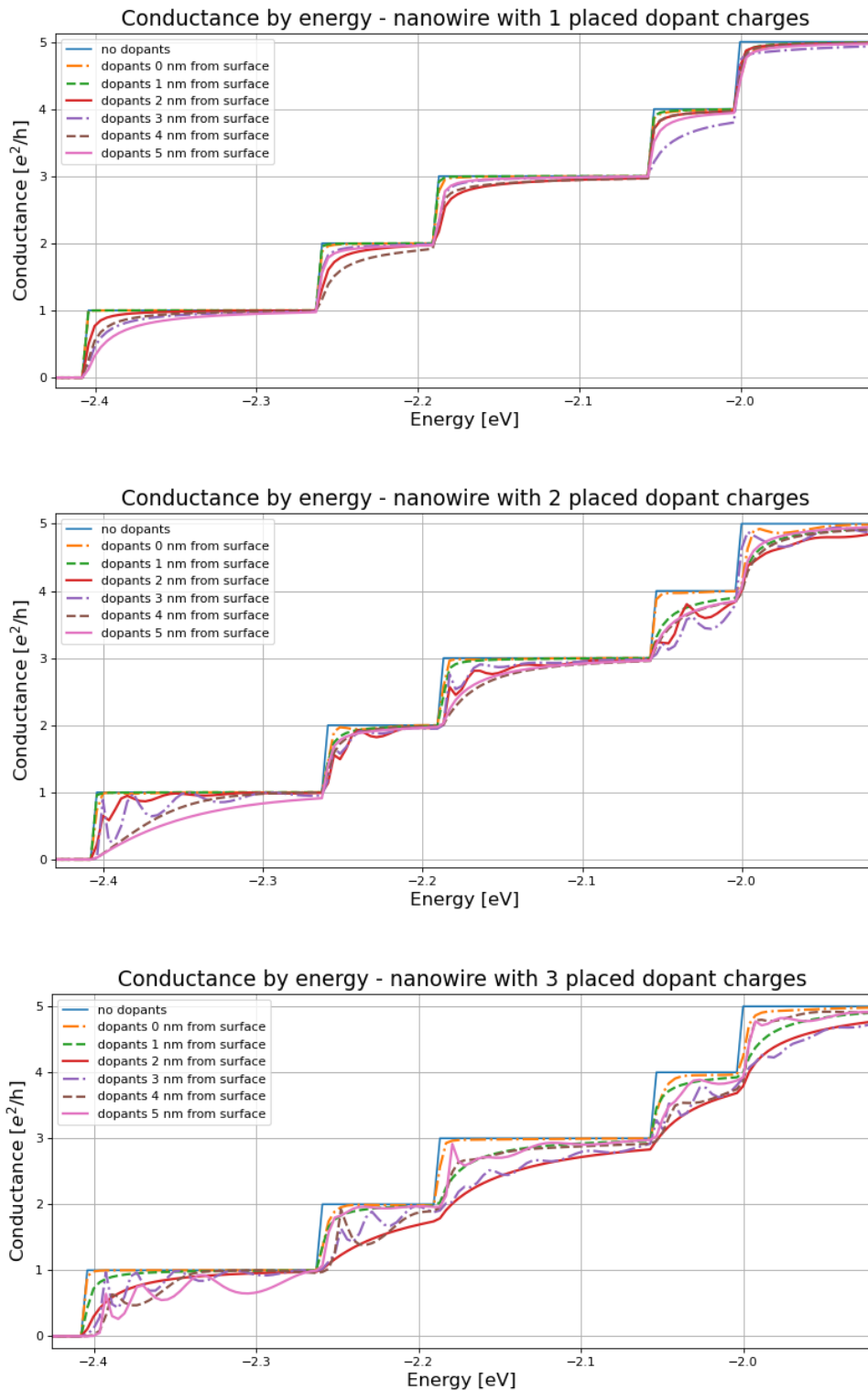


Figure A.4: Plot of conductance by energy for a nanowire with different numbers of dopant charges added. Each plot shows multiple curves with conductance data for dopant charges placed a specific distance from the surface of the nanowire. Dopant charges placed near the surface have less effect, and multiple dopant atoms can produce resonances.

## A.4 Potential Barrier Connection

One way of modelling the 'barrier' between lead and wire is by adding a literal potential barrier to the layers of the lattice directly adjacent to the leads. Some simulation runs using this method with different values of the potential are plotted below (Fig A.5).

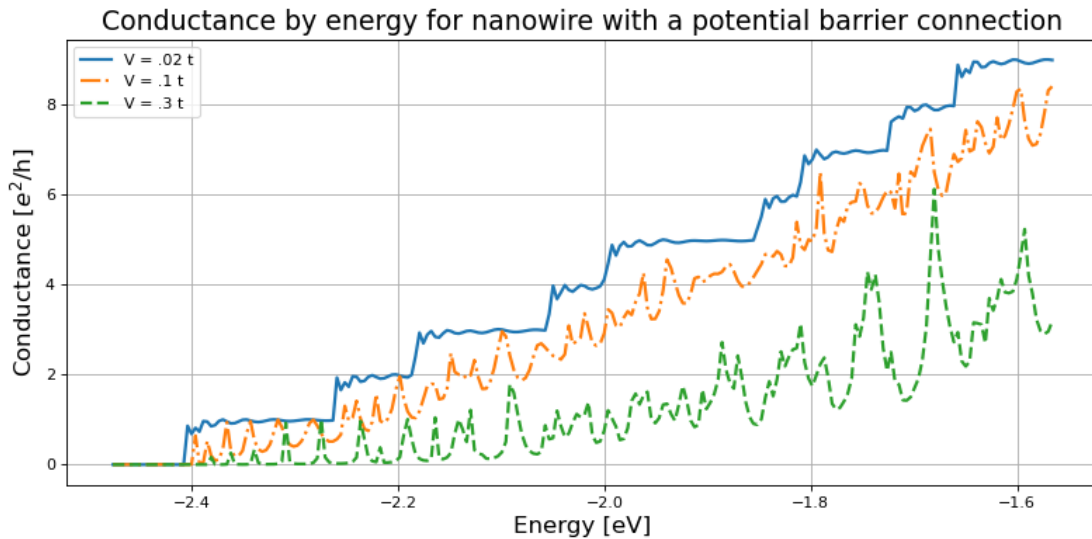


Figure A.5: Plot of conductance by energy for a nanowire with an artificial lead-wire potential barrier imposed, showing increasingly obfuscated conductance steps as the strength of the barrier is increased. Potential barrier given in simulation units of  $t$ , roughly equivalent to eV.

## A.5 The Code

The code used for these simulations and analyses is available online at '<https://bitbucket.org/AlexandrosPallaris/codeandstuff/src/master/>'.